

# Tilted Dirac cone effects and chiral symmetry breaking in a planar four-fermion model

Y. M. P. Gomes<sup>1,\*</sup> and Rudnei O. Ramos<sup>1,†</sup>

<sup>1</sup>*Departamento de Física Teórica, Universidade do Estado do Rio de Janeiro, 20550-013 Rio de Janeiro, RJ, Brazil*

We analyze the chiral symmetry breaking in a planar four-fermion model with non-null chemical potential, temperature and including the effect of the tilt of the Dirac cone. The system is modeled with a  $(2 + 1)$ -dimensional Gross-Neveu-like interaction model in the context of the generalized Weyl Hamiltonian and its phase structure is studied in the meanfield and large- $N$  approximations. Possible applications of the results obtained, e.g., in connection to graphene, are discussed. We also discuss the effect of an external magnetic field applied to the system, which can give rise to the appearance of the anomalous Hall effect and that is expected to arise in connection with two-dimensional Weyl and Dirac semimetals.

## I. INTRODUCTION

Condensed matter systems, in particular those with linearly dispersing fermionic excitations, have been serving as perfect platforms for testing predictions made by quantum field theories. This interplay between high energy physics and condensed matter has been producing new insights about the quantum phenomena. This includes since the parallel between the Ginzburg–Landau model of superconductivity and the spontaneous symmetry breaking in the Higgs sector of the standard model of particle Physics to the relation between topological insulators and axion electrodynamics, with applications, e.g., in two-dimensional systems [1–7]. The physics of graphene [8], is of particular relevance in this context, where the electrons can be treated in a quasirelativistic way through the Dirac equation in  $(2 + 1)$ -dimensions.

Although the relativistic character of the electrons in graphene is intrinsically connected with the Lorentz symmetry, this is not the case in most materials in condensed matter. In these material, the dispersion in the vicinity of band touching points, though they can be generically linear and to resemble the Weyl equation, they lack Lorentz invariance. Despite Lorentz symmetry breaking in high energy physics may emerge in specific contexts [9–15], they face strong constraints in general [16–18], Despite this, models exhibiting Lorentz symmetry breaking have been recently applied in the condensed matter area, e.g., as a path to model three-dimensional Weyl semimetals [19–22], quasi-planar organic materials and hetero-structures made of a combination of topological and normal insulators [23–26].

These new systems are described by Weyl-like Hamiltonians and, therefore, these systems have quasiparticles that behave like Weyl fermions [27]. These quasiparticles are by construction massless and are more stable against gap formation in comparison with Dirac ones. After several theoretical predictions, the first experimental measure of this kind of material [28] shed light on

the properties of the first detected Weyl semimetal (for reviews, see, e.g., Refs. [29, 30]).

We study in this work how this gapless property associated with Weyl fermions would hold against possible chiral symmetry breaking. Here, the usual Weyl Hamiltonian used in the description of Weyl semimetals [23, 24] is extended by the introducing of a four-fermion interaction. The properties of this system are then studied under the effects of both a finite chemical potential and temperature.

Let us recall that four-fermion interacting models, particularly Gross-Neveu (GN) type of models [31] in  $(2+1)$ -dimensions, are of particular interest. This is because of their simplicity and ability to capture the relevant physics of planar fermionic systems in general and, thus, these type of models have been extensively considered in the literature. These models can have either a discrete chiral symmetry,  $\psi \rightarrow \gamma_5 \psi$ , or a continuous one,  $\psi \rightarrow \exp(i\alpha\gamma_5)\psi$ . These type of models have been employed to study, e.g, low energy excitations of high-temperature superconductors [32], while analogous models with four-fermion interactions have also been used to study the quantum properties of graphene [33]. Taken as an effective low-energy description of the intrinsic physics of many relevant condensed matter systems of interest, the four-fermion models of the GN type have then served as motivation for many previous studies (see, e.g., Refs. [34–39] for examples of application). In particular, these models can make a role in understanding possible dynamical gap generation in the planar condensed matter systems, e.g., in graphene [33, 40, 41].

The aim of this paper is then to study a Weyl-like Hamiltonian, augmented by a four-fermion interaction of the GN type. We study the interplay between the characteristic anisotropy and tilting of the Dirac cone, as typically considered in these models, with both temperature and chemical potential (i.e., the effects of doping) in the phase structure of the resulting system. This study is performed in the context of the effective potential in the meanfield and large- $N$  approximation. It is expected that this study will be of interest for learning some of the analogous effects that might be important when considering fermionic quasiparticles and excitonic bound states in planar fermionic systems of relevance.

\* yurimullergomes@gmail.com

† rudnei@uerj.br

The remainder of this paper is organized as follows. In Sec. II, we show the relevant properties of two-dimensional Dirac and Weyl semimetal systems. In Sec. III, we extend the model by considering a four-fermion interaction and analyze the effective potential at the meanfield and large- $N$  level when taking into account the effects of both the anisotropy, tilting of the Dirac cone, chemical potential and temperature. In Sec. IV, we discuss some expected features for this Weyl-type model when an external magnetic field is applied to the system. Finally, in Sec. V, we give some additional discussions concerning our results and also our concluding remarks. Throughout this work, we will be considering the natural units where  $\hbar = k_B = c = 1$ .

## II. TWO-DIMENSIONAL WEYL SEMIMETALS

The generalized Hamiltonian which describes the electrons in the two-dimensional Weyl semimetal (2D WSM) is given by [23, 24],

$$H_t(\mathbf{p}) = v_F [(\mathbf{t} \cdot \mathbf{p}) \tau^0 + (\xi_x p_x) \tau^x + (\xi_y p_y) \tau^y], \quad (2.1)$$

where  $v_F$  is the Fermi velocity,  $\tau^0 = \mathbb{I}$  the  $2 \times 2$  identity matrix,  $\tau^x$  and  $\tau^y$  are the Pauli matrices,  $\mathbf{t}$  is the vector defining the tilt of the Dirac cone and  $\boldsymbol{\xi} = (\xi_x, \xi_y)$  is the vector that describes the anisotropic character of the crystalline structure. The tilt vector  $\mathbf{t}$  is related to the separation between the Dirac cones in the Weyl semimetal. A consequence of the non-null tilt term in Eq. (2.1) is that the Dirac points, denoted by  $D$  and  $D'$ , no longer coincide with the Brillouin corners  $K$  and  $K'$  (see, e.g., Ref. [24] for details and a review). In particular, type-I Weyl semimetals are characterized by  $|\mathbf{t}| < 1$ , while type-II ones by  $|\mathbf{t}| > 1$  (see Fig. 1 for an illustration). Although  $|\mathbf{t}|$  is not restricted, in order to maintain the physical meaning of the Hamiltonian Eq. (2.1), it is imposed that

$$\sqrt{\left(\frac{t_x}{\xi_x}\right)^2 + \left(\frac{t_y}{\xi_y}\right)^2} = |\tilde{\mathbf{t}}| < 1, \quad (2.2)$$

where  $|\tilde{\mathbf{t}}|$  is called the effective tilt parameter. When the condition given by Eq. (2.2) is not respected, the isoenergetic lines are no longer ellipses, but instead they are hyperboles [23, 24]. The value of  $|\tilde{\mathbf{t}}|$  depends on the material and, e.g., in quinoid-type deformed graphene [23], it is of order of  $0.6\epsilon$ , with the relative strain parameter  $\epsilon < 0.1$  for moderate deformations. The degree of freedom described by the Hamiltonian Eq. (2.1) is that of a (massless) Weyl fermion.

The Hamiltonian spectrum obtained from Eq. (2.1) is given by,

$$E(\mathbf{p}) = v_F \left[ \mathbf{t} \cdot \mathbf{p} + \lambda \sqrt{(\xi_x p_x)^2 + (\xi_y p_y)^2} \right], \quad (2.3)$$

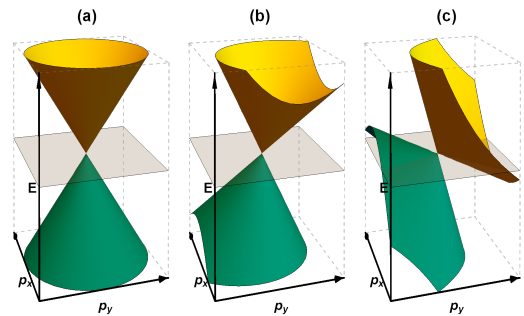


FIG. 1. Illustration of a generic Dirac cone for an isotropic Dirac semimetal (a), type I Weyl semimetal (b) and type II Weyl semimetal (c).

where  $\lambda = \pm 1$  defines the conduction and valence bands, respectively. In the untilted case  $t_x = t_y = 0$  and isotropic one,  $\xi_x = \xi_y = 1$ , we recover the spectrum of isotropic graphene. The Hamiltonian Eq. (2.1) commutes with the chirality operator given by

$$\mathcal{C} = \frac{(\xi_x p_x) \tau_x + (\xi_y p_y) \tau_y}{\sqrt{(\xi_x p_x)^2 + (\xi_y p_y)^2}}, \quad (2.4)$$

and the eigenvalues of  $\mathcal{C}$  are given by  $\alpha = \pm 1$ . Due to the two-fold degeneracy of the Dirac cones  $D$  and  $D'$ , with representative index  $\rho = \pm 1$ , the band index can be properly identified as  $\lambda = \rho\alpha$ . Taking these degeneracies into account, we can write a four-component Weyl spinor  $\psi$  and a Dirac-like Lagrangian density can be written as

$$\begin{aligned} \mathcal{L}_0 &= i\bar{\psi} \left[ (\partial_t - v_F \mathbf{t} \cdot \boldsymbol{\partial}) \gamma^0 - v_F \sum_i (\xi_i \partial_i) \gamma^i \right] \psi \\ &= i\bar{\psi} M^{\mu\nu} \gamma_\mu \partial_\nu \psi, \end{aligned} \quad (2.5)$$

where

$$\gamma^\mu = \tau^\mu \otimes \begin{pmatrix} 1 & 0 \\ 0 & -1 \end{pmatrix}, \quad (2.6)$$

$\tau^\mu = (\tau_3, i\tau_x, i\tau_y)$  and  $\bar{\psi} = \psi^\dagger \gamma^0$ . The  $\gamma$ -matrices respect the algebra  $\{\gamma^\mu, \gamma^\nu\} = 2\eta^{\mu\nu}$  (for details of this representation for fermions in  $(2+1)$ -dimensions see, e.g., Ref. [42]). We also have that

$$M^{\mu\nu} = \begin{pmatrix} 1 & -v_F t_x & -v_F t_y \\ 0 & -v_F \xi_x & 0 \\ 0 & 0 & -v_F \xi_y \end{pmatrix}. \quad (2.7)$$

One should note that  $M^{\mu\nu}$  contains the parameters that explicitly break the Lorentz symmetry. Note also that we do not introduce the two-fold spin-degeneracy here and, in case of interest, we have to double the spinors  $\psi \rightarrow \psi_s$  for  $s = \pm 1$ . It is easy to show that the Lagrangian density Eq. (2.5) has a discrete chiral symmetry given by  $\psi \rightarrow \gamma_5 \psi$  and  $\bar{\psi} \rightarrow -\bar{\psi} \gamma_5$  with [42]

$$i\gamma_5 = \begin{pmatrix} 0 & \mathbb{I} \\ -\mathbb{I} & 0 \end{pmatrix}. \quad (2.8)$$

Though there are some different ways for adding a mass term in the Lagrangian density Eq. (2.5) breaking the chiral symmetry [42], the simpler is the mass term  $\bar{\psi}\psi$ . In particular, this mass term can be generated dynamically once the model given by Eq. (2.5) is extended to include a four-fermion interaction of the GN-type. This extension is considered next.

### III. EXTENDING THE MODEL WITH A FOUR-FERMION INTERACTION

For the propose of analyzing the metal-insulator phase transition in the 2D WSM, the Lagrangian density Eq. (2.5) is extended to include a four-fermion interaction,

$$\mathcal{L} = i\bar{\psi}M^{\mu\nu}\gamma_{\mu}\partial_{\nu}\psi + \frac{\lambda v_F}{2N}(\bar{\psi}\psi)^2, \quad (3.1)$$

where  $\psi$  is a fermionic field with  $N$  flavors (the sum over the flavors implicit) and  $\lambda$  is the coupling constant. Note

that the Lagrangian density Eq. (3.1) is still invariant under the discrete chiral symmetry, unless  $\langle\bar{\psi}\psi\rangle \neq 0$ . Introducing an auxiliary field  $\sigma$ , the Lagrangian density Eq. (3.1) can be rewritten as

$$\mathcal{L} = \bar{\psi}(iM^{\mu\nu}\gamma_{\mu}\partial_{\nu} - \sigma)\psi - \frac{N}{2v_F\lambda}\sigma^2. \quad (3.2)$$

By integration of the fermionic degree of freedom in the meanfield approximation, where  $\sigma_c \equiv \langle\sigma\rangle$  is a constant background field, the effective potential for  $\sigma_c$ , at one-loop order, is given by

$$V_{\text{eff}} = \frac{N}{2v_F\lambda}\sigma_c^2 + \text{tr} \ln (iM^{\mu\nu}\gamma_{\mu}\partial_{\nu} - \sigma_c). \quad (3.3)$$

Writing Eq. (3.3) in Euclidean momentum spacetime and taking the trace, we find that

$$V_{\text{eff}} = \frac{N}{2v_F\lambda}\sigma_c^2 - 2NT \sum_{n=-\infty}^{+\infty} \int \frac{d^2p}{(2\pi)^2} \ln [(\omega_n + iv_F\mathbf{t} \cdot \mathbf{p} + i\mu)^2 + v_F^2(\boldsymbol{\xi} \cdot \mathbf{p})^2 + \sigma_c^2]. \quad (3.4)$$

where  $\omega_n = (2n + 1)\pi/\beta$  (with  $n \in \mathbb{Z}$ ,  $\beta = 1/T$  and  $T$  is the temperature of the system) are the Matsubara's frequencies for fermions and  $\mu$  is the chemical potential. Note that the chemical potential can be interpreted as to account for the extra density of electrons that is supplied to the system by the dopants and, hence, it is directly related to the doping concentration. It is also worth pointing out that Eq. (3.4) is an exact result in the large- $N$

approximation [42]. Even though for practical purposes  $N$  is finite (e.g., in graphene  $N = 2$ ), we will assume that Eq. (3.4) still provides a sufficiently good approximation as generally assumed in these four-fermion type of models [34–37].

After summing over the Matsubara's frequencies in Eq. (3.4), we find that the effective potential is given by

$$V_{\text{eff}}(\sigma_c, \mu, T) = \frac{N}{2v_F\lambda}\sigma_c^2 - 2N \int \frac{d^2p}{(2\pi)^2} \left\{ E_{\sigma} + \frac{1}{\beta} \ln [1 + e^{-\beta(E_{\sigma} + \mu)}] + \frac{1}{\beta} \ln [1 + e^{-\beta(E_{\sigma} - \mu)}] \right\}, \quad (3.5)$$

where

$$E_{\sigma} = v_F\mathbf{t} \cdot \mathbf{p} + \sqrt{v_F^2\tilde{\mathbf{p}}^2 + \sigma_c^2}, \quad (3.6)$$

with  $\tilde{\mathbf{p}}^2 = \tilde{p}_x^2 + \tilde{p}_y^2 \equiv (\boldsymbol{\xi} \cdot \mathbf{p})^2$ .

The so-called gap equation is given by

$$\left. \frac{\partial V_{\text{eff}}}{\partial \sigma_c} \right|_{\sigma_c = \bar{\sigma}_c} = 0, \quad (3.7)$$

which gives

$$1 = 2\lambda v_F \int \frac{d^2p}{(2\pi)^2} \frac{1}{\sqrt{v_F^2\tilde{\mathbf{p}}^2 + \sigma_c^2}} \times \left[ 1 - \frac{1}{e^{\beta(E_{\sigma} + \mu)} + 1} - \frac{1}{e^{\beta(E_{\sigma} - \mu)} + 1} \right] \Big|_{\sigma_c = \bar{\sigma}_c}, \quad (3.8)$$

along with the trivial solution  $\bar{\sigma}_c = 0$ .

Special cases of the above equations will be analyzed next.

### A. The $T = \mu = 0$ case

Note that the effective potential Eq. (3.5) is divergent. Considering the limit  $\beta \rightarrow \infty$  and  $\mu \rightarrow 0$  in Eq. (3.5) and performing the (divergent) momentum integral with a cutoff  $\Lambda$ , we can define the renormalization condition for the four-fermion interaction  $\lambda_R$  as [35, 43]

$$\begin{aligned} \frac{1}{\lambda_R(m)} &= \frac{v_F}{N} \left. \frac{d^2 V_{\text{eff}}(\sigma_c)}{d\sigma_c^2} \right|_{\sigma_c=m} \\ &= \frac{1}{\lambda} + \frac{2m}{\pi \xi_x \xi_y v_F} - \frac{\Lambda}{\pi \xi_x \xi_y v_F}, \end{aligned} \quad (3.9)$$

where  $m$  is a regularization scale. Next, defining the renormalization invariant coupling  $\lambda_R$  as

$$\frac{1}{\lambda_R} = \frac{1}{\lambda_R(m)} - \frac{2m}{\pi \xi_x \xi_y v_F}, \quad (3.10)$$

we arrive at the renormalized effective potential as given by

$$\begin{aligned} V_{\text{eff,R}}(\sigma_c) &= \frac{N}{2v_F \lambda_R} \sigma_c^2 \\ &+ \frac{N}{3\pi \xi_x \xi_y v_F^2} |\sigma_c|^3. \end{aligned} \quad (3.11)$$

When  $\lambda_R < 0$ , the nontrivial vacuum solution of Eq. (3.11) is given by

$$\bar{\sigma}_c = \sigma_0 \equiv \frac{v_F \pi \xi_x \xi_y}{|\lambda_R|}, \quad (3.12)$$

while for  $\lambda_R > 0$  we have that  $\bar{\sigma}_c = 0$ . Note that

$$V_{\text{eff,R}}(\sigma_c = \sigma_0) = \frac{N(\pi \xi_x \xi_y)^2 v_F}{6\lambda_R^3}, \quad (3.13)$$

and, hence, Eq. (3.12) corresponds to the true minimum of the system. We can also see that the value of  $\sigma_0$  is modified by the dependence on the anisotropy constants,  $\xi_x \xi_y$ , and we recover the usual result [34, 35] in the isotropic limit:  $\xi_x, \xi_y \rightarrow 1$ . One can further notice here, in the zero temperature and zero chemical potential limits, that the tilt parameter  $\mathbf{t}$  does not contribute to the effective potential.

### B. The $T = 0$ and $\mu \neq 0$ case

At zero temperature but with a non-null chemical potential, from the effective potential Eq. (3.5) and considering Eq. (2.2), one obtains that

$$\begin{aligned} V_{\text{eff,R}}(\sigma_c, \mu) &= V_{\text{eff,R}}(\sigma_c) \\ &- 2N \int \frac{d^2 p}{(2\pi)^2} (\mu - E_\sigma) \Theta(\mu - E_\sigma), \end{aligned} \quad (3.14)$$

where  $\Theta(x)$  is the standard Heaviside function. For a small tilt parameter,  $|\tilde{\mathbf{t}}| \ll 1$ , we can find for Eq. (3.14) the approximated result

$$\begin{aligned} V_{\text{eff,R}}(\sigma_c, \mu) &= V_{\text{eff,R}}(\sigma_c) - \frac{N}{2\pi \xi_x \xi_y v_F^2} \Theta(\mu^2 - \sigma_c^2) \\ &\times \left[ \frac{1}{3} (\mu^3 - 3\sigma_c^2 \mu + 2|\sigma_c|^3) + \frac{1}{2} |\tilde{\mathbf{t}}|^2 \mu (\mu^2 - \sigma_c^2) \right] \\ &+ \mathcal{O}(|\tilde{\mathbf{t}}|^4). \end{aligned} \quad (3.15)$$

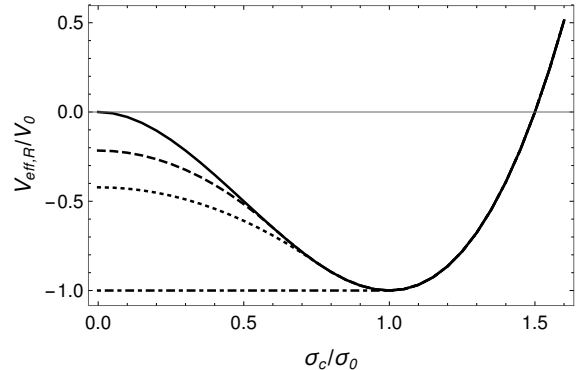


FIG. 2. Normalized plot of the renormalized effective potential at zero temperature, Eq. (3.14), in units of  $V_0 \equiv N\sigma_0^3/(6\pi v_F^2 \xi_x \xi_y)$ , for  $\mu = 0$ ,  $|\tilde{\mathbf{t}}| = 0$  (solid line),  $\mu = 0.6\sigma_0$ ,  $|\tilde{\mathbf{t}}| = 0$  (dashed line),  $\mu = 0.6\sigma_0$ ,  $|\tilde{\mathbf{t}}| = 0.6$  (dotted line) and for  $\mu = 0.6\sigma_0$ ,  $|\tilde{\mathbf{t}}| = 0.8$  (dash-dotted line).

The Eq. (3.15) shows that the effect of the tilde parameter is to enhance the chemical potential. This is confirmed by the result shown in Fig. (2), which shows the result of Eq. (3.14) for the effective potential as a function of the gap parameter  $\bar{\sigma}_c$  for some representative values of  $\mu$  and  $|\tilde{\mathbf{t}}|$ . It is then seen that the tilt parameter has the effect of improving the stability of the chiral symmetry in the planar fermionic model. This can be confirmed by determining the critical point  $\mu_c$  for which the chiral symmetry gets restored. Let us recall that at vanishing tilt parameter,  $|\tilde{\mathbf{t}}| = 0$ , the chiral symmetry is restored through a first-order phase transition [44–46]. The critical point is then determined by the condition  $V_{\text{eff,R}}(\sigma_c = 0, \mu_c) = V_{\text{eff,R}}(\sigma_c = \sigma_0, \mu_c)$ . Using Eq. (3.14), we then find that the critical chemical potential as a function of the tilt parameter is given by

$$\mu_c = (1 - |\tilde{\mathbf{t}}|^2)^{1/2} \sigma_0. \quad (3.16)$$

At the critical value  $\mu_c$ , the potential loses its non-trivial minimum, i.e.,  $\bar{\sigma}_c(\mu = \mu_c) = 0$ . The critical value  $\mu_c$  as a function of the tilt parameter is shown in Fig. 3. For  $|\tilde{\mathbf{t}}| = 0$  we recover the known result  $\mu_c = \sigma_0$ . The

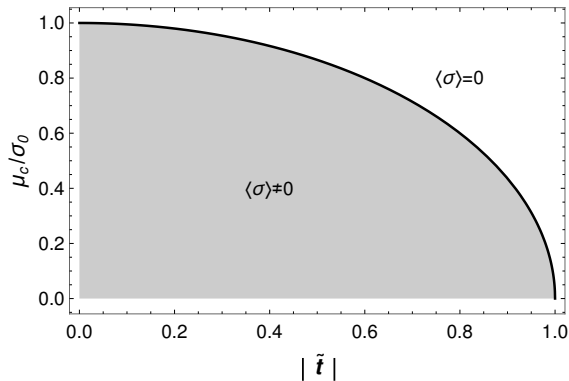


FIG. 3. The critical chemical potential  $\mu_c$  (in units of  $\sigma_0$ ) as a function of  $|\tilde{\mathbf{t}}|$ .

result for the critical  $\mu_c$  shown in Eq. (3.16) clearly shows that in the presence of a non-null tilt parameter, the gap  $\bar{\sigma}_c$  will vanish at a smaller doping and, hence, facilitating the chiral symmetry restoration.

Note that the tilt parameter also affects the Fermi momentum, which is now given by

$$\tilde{p}_F = \frac{\sqrt{\mu^2 - [1 - |\tilde{\mathbf{t}}|^2 \cos^2(\theta)] \bar{\sigma}_c^2 - \mu |\tilde{\mathbf{t}}| \cos(\theta)}}{v_F [1 - |\tilde{\mathbf{t}}|^2 \cos^2(\theta)]}, \quad (3.17)$$

where  $\theta$  is the angle between  $\mathbf{p}_F$  and the tilt vector  $\mathbf{t}$ . We see that for  $-\pi/2 < \theta < \pi/2$ , the tilt parameter acts towards increasing the Fermi surface. This is also reflected on the behavior of the charge density  $n$ , which is defined as

$$n = - \left. \frac{\partial V_{\text{eff,R}}}{\partial \mu} \right|_{\sigma_c = \bar{\sigma}_c}, \quad (3.18)$$

and, using Eq. (3.14), it gives the result

$$n(\sigma_c, \mu) = N \frac{\mu^2 - (1 - |\tilde{\mathbf{t}}|^2) \bar{\sigma}_c^2}{2\pi \xi_x \xi_y v_F^2 (1 - |\tilde{\mathbf{t}}|^2)^{3/2}} \Theta[\mu^2 - (1 - |\tilde{\mathbf{t}}|^2) \bar{\sigma}_c^2]. \quad (3.19)$$

At the critical value  $\mu_c$  given by Eq. (3.16) we have that  $n(\bar{\sigma}_c = 0, \mu_c) = N \sigma_0^2 / (2\pi \xi_x \xi_y v_F^2 \sqrt{1 - |\tilde{\mathbf{t}}|^2})$ , which is always larger than in the absence of the tilt parameter. This is explicitly seen also in Fig. 4, where Eq. (3.19) is shown as a function of the chemical potential, for a non-tilted Dirac cone case and also for a tilted one. The discontinuity is the characteristic behavior due to the first-order phase transition at the critical point  $\mu_c$ .

### C. $T \neq 0, \mu \neq 0$

Let us now analyze the case where both temperature and chemical potential are included and, hence, the effective potential is given by Eq. (3.5). The critical curve for

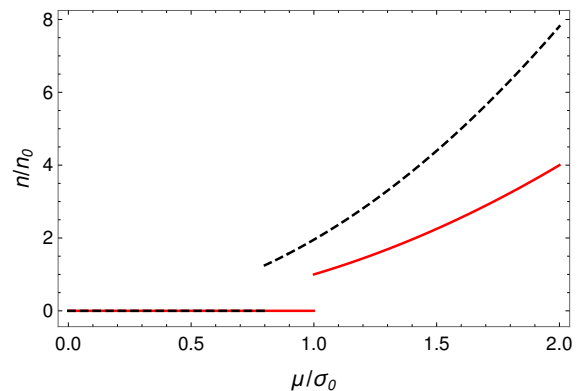


FIG. 4. Density at zero temperature (in units of  $n_0 \equiv N \sigma_0^2 / (2\pi v_F^2 \xi_x \xi_y)$ ) as a function of the chemical potential for  $|\tilde{\mathbf{t}}| = 0$  (solid line) and for  $|\tilde{\mathbf{t}}| = 0.6$  (dashed line).

which  $\bar{\sigma}_c(T_c, \mu_c) = 0$  is obtained from the gap equation Eq. (3.8),

$$\sigma_0 + \frac{\mu_c - 2T_c \ln(e^{\mu_c/T_c} + 1)}{(1 - |\tilde{\mathbf{t}}|^2)^{1/2}} = 0, \quad (3.20)$$

which reproduces the result Eq. (3.16) in the zero temperature limit, while at zero chemical potential it gives

$$T_c = \sqrt{1 - |\tilde{\mathbf{t}}|^2} \frac{\sigma_0}{2 \ln 2}. \quad (3.21)$$

Thus, both  $T_c$  and  $\mu_c$  are suppressed by the tilt parameter, exhibiting again the tendency of facilitating the chiral symmetry restoration when  $|\tilde{\mathbf{t}}| \neq 0$ . The behavior of  $T_c$  at  $\mu = 0$  and as a function of the tilt parameter is shown in Fig. 5

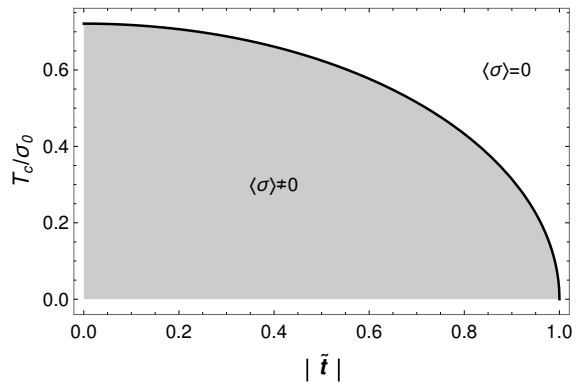


FIG. 5. The critical temperature as a function of  $|\tilde{\mathbf{t}}|$  for  $\mu = 0$ .

The overall behavior of the critical curve obtained from Eq. (3.20) is shown in Fig. 6.

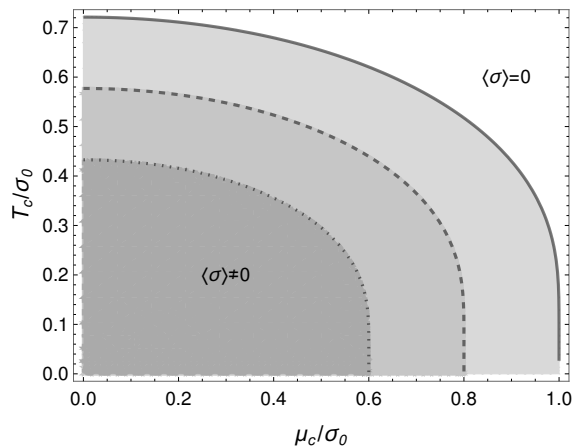


FIG. 6. Critical curve  $\bar{\sigma}_c(\mu_c, T_c) = 0$  for  $|\tilde{\mathbf{t}}| = 0$  (solid line) and for  $|\tilde{\mathbf{t}}| = 0.6$  (dashed line) and  $|\tilde{\mathbf{t}}| = 0.8$  (dotted line).

#### IV. THE EFFECT OF AN EXTERNAL MAGNETIC FIELD

Let us now briefly discuss some possible consequences of adding an external magnetic field to the system. Since the electrons in the 2D Dirac (Weyl) semimetal are charged, we can add a coupling with the electromagnetic sector through the minimal coupling, i.e.,  $\partial_\mu \rightarrow \nabla_\mu = \partial_\mu - ieA_\mu$ . The Lagrangian density Eq. (2.5) is then modified as follows,

$$\begin{aligned} \mathcal{L}_0 &= \bar{\psi} (iM^{\mu\nu} \gamma_\mu \nabla_\nu) \psi \\ &= \bar{\psi} (iM^{\mu\nu} \gamma_\mu \partial_\nu) \psi + e\bar{\psi} \gamma_\mu \psi \tilde{A}^\mu, \end{aligned} \quad (4.1)$$

where we have defined an effective electromagnetic potential  $\tilde{A}_\mu$  with components

$$\tilde{A}_0 = A_0 - v_F \mathbf{t} \cdot \mathbf{A}, \quad \tilde{A}_i = \xi_{ij} A_j, \quad i = x, y. \quad (4.2)$$

where  $\xi_{ij} = \xi_i \delta_{ij}$ . Thus, by considering the 2D system in the  $(x, y)$  plane and in the presence an external and constant magnetic field  $\mathbf{B}$ , we can, without loss of generality, choose a gauge such that the external four-vector potential is given by  $A_0 = 0$  and  $\mathbf{A}_{3D} = -\frac{1}{2} x \hat{\mathbf{x}} \times \mathbf{B}$ , which leads to a magnetic field component perpendicular to the system's plane,  $B_\perp \equiv B_z$  and another component that is parallel to the plane,  $B_\parallel \equiv B_y$ . Hence, from the tilt vector defined by  $\mathbf{t} = (t_x, t_y, 0)$ , it is easy to see that Eq. (4.2) can be expressed in the form,

$$\tilde{A}_0 = -\frac{1}{2} v_F x \hat{\mathbf{x}} \cdot (\mathbf{B} \times \mathbf{t}) = \frac{1}{2} v_F x t_x B_\perp. \quad (4.3)$$

Therefore,  $B_\perp$  generates a non-null contribution to the time-component of the effective vector potential  $\tilde{A}_0$  and, thus, the magnetic field will act analogous to an effective external electric field, with magnitude  $\tilde{\mathbf{E}}_i = \frac{1}{2} v_F \xi_{ij} (\mathbf{B} \times \mathbf{t})_j$ . Besides of this, the anisotropy in the spatial direction modifies the magnetic field in the perpendicular direction,  $\tilde{B}_\perp = \xi_x \xi_y B_\perp$ , while in the parallel direction,

$\tilde{B}_\parallel = \xi_y B_\parallel$ . Thus, the external magnetic field generates an electrochemical potential given by

$$\tilde{\mu}_s = \mu + \frac{e}{2} v_F x \hat{\mathbf{x}} \cdot (\mathbf{B} \times \mathbf{t}) + \frac{s}{2} g \mu_B |\tilde{\mathbf{B}}|, \quad (4.4)$$

where  $g$  is the spectroscopic Landé factor of the electrons ( $g \approx 2$  in graphene),  $s = \pm 1$  and  $\mu_B$  is the Bohr magneton.

We can then see that the tilting of the Dirac cone and the anisotropy generate two effects. Firstly, the combination of a external magnetic field and the tilt vector  $\mathbf{t}$  generates a non-null chemical affinity  $A_i \propto -\nabla_i \mu_s = e(\tilde{\mathbf{E}})_i = \frac{e}{2} v_F B_\perp \xi_{ij} \epsilon^{jk} t_k$  and, therefore, by Onsager reciprocal relations, it will generate a current perpendicular to  $\mathbf{t}$ . This current will be proportional to  $\Phi = \int d^2x B_\perp$ . Hence, one can affirm that the 2D Dirac (Weyl) semimetal will have an anomalous Hall effect [47]. Secondly, the magnetic field coupling generates an anisotropic Zeeman effect and, therefore, it can be interpreted as an effective giromagnetic term dependent on the direction of the  $\mathbf{B}_\parallel$  field. It would be worthwhile to further explore these effects in applications of these type of planar models when subjected to an external magnetic field and which we leave as a future work.

#### V. CONCLUSIONS

In this work we have analyzed the problem of chiral symmetry breaking in a planar four-fermion model when considered in the context of the generalized Weyl Hamiltonian. The Gross-Neveu-like four-fermion interaction provides a way to study the chiral symmetry breaking in the model. The free Hamiltonian that we have employed in this study was the generalized Weyl one, which includes the anisotropies and the explicit tilting of the Dirac cone. We have then studied how the tilting of the Dirac cone, parameterized by the so-called effective tilt parameter  $|\tilde{\mathbf{t}}|$ , affects the chiral phase transition as a function of both chemical potential (e.g., doping) and finite temperature. Both the critical temperature and critical chemical potential decrease by a factor  $\sqrt{1 - |\tilde{\mathbf{t}}|^2}$  with respect to the untilted case. Thus, the tilt parameter suppresses the chiral symmetry breaking, easing its restoration. At the same time, the chiral order parameter  $\sigma_0$ , which introduces a mass gap in the system, is affected by the anisotropy through the geometric mean Fermi velocity,  $v_F^* = \sqrt{\xi_x \xi_y} v_F$ .

The difference between the effective Fermi velocity  $v_F^*$  and the usual one in fully isotropic materials (considering the case of, e.g., graphene, where  $v_F \approx c/300$ ) can alter significantly the critical temperature and critical chemical potential. This is because the dependence of  $v_F^*$  on the anisotropies does not have a strong physical bound such as the one observed by the tilt parameter  $|\tilde{\mathbf{t}}|$  and given by Eq. (2.2).

It is worth to provide some estimates, even though that they might be rough ones, based on results ob-

tained from some current planar systems of interest, particularly organic conductors. For instance, in a recent study with a two-dimensional organic conductor [48]  $\alpha - (\text{BEDT-TTF})_2\text{I}_3$ , the tilt vector  $\mathbf{t}$  and anisotropy  $\boldsymbol{\xi}$  vector can be estimated as given, respectively, by  $\mathbf{t} \simeq (-1.7, 0.3) \times 10^{-4}$  and  $\boldsymbol{\xi} \simeq (2.3, 2.4) \times 10^{-4}$ , where we have assumed a graphene like Fermi velocity as a base one (i.e., in the isotropic case). Thus, the effective Fermi velocity is  $v_F^* \approx 0.02v_F$  and the effective tilt parameter can be estimated as  $|\tilde{\mathbf{t}}| \approx 0.76$ . Therefore, from Eqs. (3.16) and (3.21), the critical chemical potential and critical temperature get both reduced by a factor  $\sqrt{1 - |\tilde{\mathbf{t}}|^2 \xi_x \xi_y} \approx 3.6 \times 10^{-8}$  with respect to the untilted and isotropic critical values. This is quite a substantial reduction. This is to be contrasted with the case of Quinoid-type graphene under uniaxial strain [23], where  $v_F^* \approx v_F$  and the critical temperature and chemical potential of this system can be estimated to decrease by a factor  $(1 - 0.02\epsilon^2)$ , where  $\epsilon$  is the relative strain. Given that  $\epsilon < 1$  for moderate strain, this leads to a much smaller suppression of  $\mu_c$  and  $T_c$ . Thus, our results indicate that planar organic conductors can remain gapless down to very small temperatures and dopings as a result of the combined effects of anisotropy and Dirac cone tilt.

Lastly, we have shown that the planar fermion sys-

tem that we have studied will respond to an external magnetic field differently in the absence and presence of the Dirac cone tilt. There will be an anomalous Hall effect and its magnitude is proportional to the Lorentz-violating parameters  $\boldsymbol{\xi}$  and  $\mathbf{t}$ . This effect changes the effective chemical potential and a current perpendicular to  $\mathbf{t}$  appears. The anomalous Hall effect [47] is related to the emergence of this unusual current  $\mathbf{j} \propto \mathbf{t} \times \mathbf{B}$ . In the model case we have studied, this effect comes from the explicit Lorentz-violating structure of the matrix  $M^{\mu\nu}$  in Eq. (4.1). It generates a non-constant contribution to the chemical potential, which is an explicitly character of non-equilibrium systems and which can lead to interesting features in the study of transport phenomena. These and other features found here as a consequence of this study will be analyzed in more details a future work.

## ACKNOWLEDGMENTS

Y.M.P.G. is supported by a postdoctoral grant from Fundação Carlos Chagas Filho de Amparo à Pesquisa do Estado do Rio de Janeiro (FAPERJ). R.O.R. is partially supported by research grants from Conselho Nacional de Desenvolvimento Científico e Tecnológico (CNPq), Grant No. 302545/2017-4, and from FAPERJ, Grant No. E-26/202.892/2017.

- 
- [1] J. Yu, R. Roiban, S. K. Jian and C. X. Liu, “Finite-Scale Emergence of 2+1D Supersymmetry at First-Order Quantum Phase Transition,” *Phys. Rev. B* **100**, no.7, 075153 (2019) doi:10.1103/PhysRevB.100.075153 [arXiv:1902.07407 [cond-mat.str-el]].
- [2] P. Gao and H. Liu, “Emergent Supersymmetry in Local Equilibrium Systems,” *JHEP* **01**, 040 (2018) doi:10.1007/JHEP01(2018)040 [arXiv:1701.07445 [hep-th]].
- [3] A. Rahmani, X. Zhu, M. Franz and I. Affleck, “Emergent Supersymmetry from Strongly Interacting Majorana Zero Modes,” *Phys. Rev. Lett.* **115**, no.16, 166401 (2015) [erratum: *Phys. Rev. Lett.* **116**, no.10, 109901 (2016)] doi:10.1103/PhysRevLett.115.166401 [arXiv:1504.05192 [cond-mat.str-el]].
- [4] T. Grover, D. N. Sheng and A. Vishwanath, “Emergent Space-Time Supersymmetry at the Boundary of a Topological Phase,” *Science* **344**, no.6181, 280-283 (2014) doi:10.1126/science.1248253 [arXiv:1301.7449 [cond-mat.str-el]].
- [5] L. D. Bernal, P. Gaete, Y. P. M. Gomes and J. A. Helayël-Neto, “Lorentz-symmetry violating physics in a supersymmetric scenario in (2 + 1)-D,” *EPL* **129**, no.1, 11005 (2020) doi:10.1209/0295-5075/129/11005 [arXiv:1912.00523 [hep-th]].
- [6] L. Wu, M. Salehi, N. Koirala, J. Moon, S. Oh and N. P. Armitage, “Quantized Faraday and Kerr rotation and axion electrodynamics of the surface states of three-dimensional topological insulators,” *Science* **354**, 1124 (2016) doi:10.1126/science.aaf5541 [arXiv:1603.04317 [cond-mat.mes-hall]].
- [7] S. R. Coleman, R. Jackiw and H. D. Politzer, “Spontaneous Symmetry Breaking in the O(N) Model for Large N\*,” *Phys. Rev. D* **10**, 2491 (1974) doi:10.1103/PhysRevD.10.2491
- [8] K. S. Novoselov, A. K. Geim, S. V. Morozov, D. Jiang, M. I. Katsnelson, I. V. Grigorieva, S. V. Dubonos and A. A. Firsov, “Two-dimensional gas of massless Dirac fermions in graphene,” *Nature* **438**, 197 (2005) doi:10.1038/nature04233 [arXiv:cond-mat/0509330 [cond-mat.mes-hall]].
- [9] V. A. Kostelecky and S. Samuel, “Spontaneous Breaking of Lorentz Symmetry in String Theory,” *Phys. Rev. D* **39**, 683 (1989) doi:10.1103/PhysRevD.39.683
- [10] I. Mocioiu, M. Pospelov and R. Roiban, “Breaking CPT by mixed noncommutativity,” *Phys. Rev. D* **65**, 107702 (2002) doi:10.1103/PhysRevD.65.107702 [arXiv:hep-ph/0108136 [hep-ph]].
- [11] N. E. Mavromatos, “Probing Lorentz Violating (Stringy) Quantum Space-Time Foam,” *AIP Conf. Proc.* **1196**, no.1, 169 (2009) doi:10.1063/1.3284380 [arXiv:0909.2319 [hep-th]].
- [12] N. E. Mavromatos, “Lorentz Invariance Violation from String Theory,” *PoS QG-PH*, 027 (2007) doi:10.22323/1.043.0027 [arXiv:0708.2250 [hep-th]].
- [13] D. Colladay and V. A. Kostelecky, “CPT violation and the standard model,” *Phys. Rev. D* **55**, 6760-6774 (1997) doi:10.1103/PhysRevD.55.6760 [arXiv:hep-ph/9703464 [hep-ph]].

- [14] D. Colladay and V. A. Kostelecky, “Lorentz violating extension of the standard model,” *Phys. Rev. D* **58**, 116002 (1998) doi:10.1103/PhysRevD.58.116002 [arXiv:hep-ph/9809521 [hep-ph]].
- [15] V. A. Kostelecky and N. Russell, “Data Tables for Lorentz and CPT Violation,” *Rev. Mod. Phys.* **83**, 11-31 (2011) doi:10.1103/RevModPhys.83.11
- [16] D. Mattingly, “Modern tests of Lorentz invariance,” *Living Rev. Rel.* **8**, 5 (2005) doi:10.12942/lrr-2005-5 [arXiv:gr-qc/0502097 [gr-qc]].
- [17] V. A. Kostelecky and N. Russell, “Data Tables for Lorentz and CPT Violation,” [arXiv:0801.0287 [hep-ph]].
- [18] V. A. Kostelecký and A. J. Vargas, “Lorentz and CPT tests with hydrogen, antihydrogen, and related systems,” *Phys. Rev. D* **92**, no.5, 056002 (2015) doi:10.1103/PhysRevD.92.056002 [arXiv:1506.01706 [hep-ph]].
- [19] A. G. Grushin, “Consequences of a condensed matter realization of Lorentz violating QED in Weyl semi-metals,” *Phys. Rev. D* **86**, 045001 (2012) doi:10.1103/PhysRevD.86.045001 [arXiv:1205.3722 [hep-th]].
- [20] S. Tchoumakov, M. Civelli, and M. O. Goerbig, “Magnetic field-induced relativistic properties in type-I and type-II Weyl semimetals,” *Phys. Rev. Lett.* **117**, 086402 (2016).
- [21] A. A. Soluyanov, D. Gresch, Z. Wang, Q. Wu, M. Troyer, X. Dai, and B. Andrei Bernevig, “Type-II weyl semimetals,” *Nature* **527**, 495–498 (2015).
- [22] X. Wan, et al., “Topological semimetal and Fermi-arc surface states in the electronic structure of pyrochlore iridates,” *Phys. Rev. B* **83**, 205101 (2011).
- [23] M. O. Goerbig, et al., “Tilted anisotropic Dirac cones in quinoid-type graphene and  $\alpha$ -(BEDT-TTF) $_2$ I $_3$ ,” *Phys. Rev. B* **78**, 045415 (2008).
- [24] M. O. Goerbig, “Electronic properties of graphene in a strong magnetic field,” *Rev. Mod. Phys.* **83**, 1193 (2011).
- [25] A. Kobayashi, et. al., “Massless fermions in organic conductor,” *Journal of the Physical Society of Japan* **76**, 034711 (2007).
- [26] S. Katayama, A. Kobayashi and Y. Suzumura, “Pressure-induced zero-gap semiconducting state in organic conductor  $\alpha$ -(BEDT-TTF) 2I3 salt,” *Journal of the Physical Society of Japan* **75**, 054705 (2006).
- [27] H. Weyl, “Elektron und gravitation. I,” *Zeitschrift für Physik* **56**, 330-352 (1929).
- [28] S. Y. Xu, I. Belopolski, N. Alidoust, M. Neupane, G. Bian, C. Zhang, R. Sankar, G. Chang, Z. Yuan and C. C. Lee, *et al.* “Discovery of a Weyl Fermion semimetal and topological Fermi arcs,” *Science* **349**, 613-617 (2015) doi:10.1126/science.aaa9297 [arXiv:1502.03807 [cond-mat.mes-hall]].
- [29] N. P. Armitage, E. J. Mele and A. Vishwanath, “Weyl and Dirac Semimetals in Three Dimensional Solids,” *Rev. Mod. Phys.* **90**, no.1, 015001 (2018) doi:10.1103/RevModPhys.90.015001 [arXiv:1705.01111 [cond-mat.str-el]].
- [30] B. Yan and C. Felser, “Topological Materials: Weyl Semimetals,” *Ann. Rev. Condensed Matter Phys.* **8**, 337-354 (2017) doi:10.1146/annurev-conmatphys-031016-025458 [arXiv:1611.04182 [cond-mat.mtrl-sci]].
- [31] D. J. Gross and A. Neveu, “Dynamical Symmetry Breaking in Asymptotically Free Field Theories,” *Phys. Rev. D* **10**, 3235 (1974) doi:10.1103/PhysRevD.10.3235
- [32] W. V. Liu, “Parity breaking and phase transition induced by a magnetic field in high T(c) superconductors,” *Nucl. Phys. B* **556**, 563-572 (1999) doi:10.1016/S0550-3213(99)00309-0 [arXiv:cond-mat/9808134 [cond-mat]].
- [33] J. E. Drut and D. T. Son, “Renormalization group flow of quartic perturbations in graphene: Strong coupling and large-N limits,” *Phys. Rev. B* **77**, 075115 (2008) doi:10.1103/PhysRevB.77.075115 [arXiv:0710.1315 [cond-mat.str-el]].
- [34] H. Caldas and R. O. Ramos, “Magnetization of planar four-fermion systems,” *Phys. Rev. B* **80**, 115428 (2009) doi:10.1103/PhysRevB.80.115428 [arXiv:0907.0723 [cond-mat.soft]].
- [35] R. O. Ramos and P. H. A. Manso, “Chiral phase transition in a planar four-fermion model in a tilted magnetic field,” *Phys. Rev. D* **87**, no.12, 125014 (2013) doi:10.1103/PhysRevD.87.125014 [arXiv:1303.5463 [hep-ph]].
- [36] K. G. Klimenko and R. N. Zhokhov, “Magnetic catalysis effect in the (2+1)-dimensional Gross-Neveu model with Zeeman interaction,” *Phys. Rev. D* **88**, no.10, 105015 (2013) doi:10.1103/PhysRevD.88.105015 [arXiv:1307.7265 [hep-ph]].
- [37] D. Ebert, K. G. Klimenko, P. B. Kolmakov and V. C. Zhukovsky, “Phase transitions in hexagonal, graphene-like lattice sheets and nanotubes under the influence of external conditions,” *Annals Phys.* **371**, 254-286 (2016) doi:10.1016/j.aop.2016.05.001 [arXiv:1509.08093 [cond-mat.mes-hall]].
- [38] D. Ebert, T. G. Khunjua, K. G. Klimenko and V. C. Zhukovsky, “Competition and duality correspondence between chiral and superconducting channels in ( 2+1 )-dimensional four-fermion models with fermion number and chiral chemical potentials,” *Phys. Rev. D* **93**, no.10, 105022 (2016) doi:10.1103/PhysRevD.93.105022 [arXiv:1603.00357 [hep-th]].
- [39] L. Fernández, V. Alves, M. Gomes, L. O. Nascimento and F. Peña, “Influence of the four-fermion interactions in a (2+1)D massive electron system,” *Phys. Rev. D* **103**, no.10, 105016 (2021) doi:10.1103/PhysRevD.103.105016 [arXiv:2103.07979 [hep-th]].
- [40] V. Juricic, I. F. Herbut and G. W. Semenoff, “Coulomb interaction at the metal-insulator critical point in graphene,” *Phys. Rev. B* **80**, 081405 (2009) doi:10.1103/PhysRevB.80.081405 [arXiv:0906.3513 [cond-mat.str-el]].
- [41] I. F. Herbut, V. Juricic and O. Vafek, “Relativistic Mott criticality in graphene,” *Phys. Rev. B* **80**, 075432 (2009) doi:10.1103/PhysRevB.80.075432 [arXiv:0904.1019 [cond-mat.str-el]].
- [42] B. Rosenstein, B. Warr and S. H. Park, “Dynamical symmetry breaking in four Fermi interaction models,” *Phys. Rept.* **205**, 59-108 (1991) doi:10.1016/0370-1573(91)90129-A
- [43] A. S. Vshivtsev, K. G. Klimenko and B. V. Magnitsky, “Vacuum structure of the  $(\bar{\psi}\psi)^2$  model, accounting for the magnetic field and chemical potential,” *Theor. Math. Phys.* **106**, 319-327 (1996) doi:10.1007/BF02071476
- [44] K. G. Klimenko, “Phase Structure of Generalized Gross-Neveu Models,” *Z. Phys. C* **37**, 457 (1988) doi:10.1007/BF01578141
- [45] B. Rosenstein, B. J. Warr and S. H. Park, “Thermodynamics of (2+1)-dimensional Four Fermi Models,” *Phys.*

- Rev. D **39**, 3088 (1989) doi:10.1103/PhysRevD.39.3088
- [46] B. Rosenstein, B. J. Warr and S. H. Park, “The Four Fermi Theory Is Renormalizable in (2+1)-Dimensions,” Phys. Rev. Lett. **62**, 1433-1436 (1989) doi:10.1103/PhysRevLett.62.1433
- [47] A.A. Burkov, “Chiral anomaly and transport in Weyl metals”, Journal of Physics: Condensed Matter, **27** (11), p. 113201 (2015).
- [48] M. Hirata, et al, “Observation of an anisotropic Dirac cone reshaping and ferrimagnetic spin polarization in an organic conductor”, Nature comm., **7** (1), p. 1-14 (2016).